Pitch Damping of Helicopter Rotor with Nonuniform Inflow

Akira Azuma* and Yoshiya Nakamura†
University of Tokyo, Tokyo, Japan

Pitch or roll damping of helicopter rotor has been experimentally studied by using model rotors in rocking motion. The rotors have articulated blades with spring constrained hinges and different combinations of Lock number, flapping hinge offset, and hinge constrained stiffness. By considering nonuniform induced velocity distribution a theoretical estimation based on the momentum and blade element theory has shown good coincidence with the experimental results. In contrast with analyses based on the vortex theory the present theory is very simple and does not require complex calculations so that the analytic evaluation and the quick estimation of the dynamic stability derivatives of rotor will be possible. The blade flapping behavior during sinusoidal rocking motion has also been analytically and experimentally analyzed and the mechanism of generation of direct damping and cross coupling moments have been clearly explained.

Nomenclature

a = lift slope of the blade airfoil
B = blade tip-loss-factor
b = number of blade of the rotor
C_M = moment coefficient of the rotor at hub
C_T = thrust coefficient
c = blade chord, m
c_l, c_d = lift and drag coefficients of the blade
g = gravity acceleration, m/sec^2
I = moment of inertia of a blade, kg m sec^2
I_s = moment of inertia of rotor system in rocking motion
i = rotor incidence with respect to the forward velocity or negative angle of attack of the tip path plane
j = imaginary = $(-1)^{1/2}$
K_1, K_2, K_3 = rotor dynamic parameters given by $K_1 = (\gamma/2)[(1/3)B^4 - (1/3)B^3 x_\beta]$, $K_2 = (\gamma/2)\{(1/3)B^3 - (1/2)B^2 x_\beta]$, $K_3 = (\gamma/2)[(1/2)B^2 - Bx_\beta]$
K_0, K_{1c}, K_{1s} = parameters expressing the nonuniformity of the induced velocity given by Eq. (3)
K_β = equivalent hinge stiffness = $\{(k_\beta/\Omega^2) + mR^2 x_\beta(\bar{x} - x_\beta)\}/I$
k_β = spring stiffness, kg/rad
m = mass of the blade, kg sec^2/m
p = rolling angular velocity, rad/sec
q = pitching angular velocity, rad/sec
R = rotor radius, m
r = radial position of the blade element, m
r_β = flapping hinge offset, m
s = Laplace transformation parameter, 1/sec
t = time, sec
U = relative velocity of the blade element with respect to air, m/sec
U_T, U_P = tangential and normal components of U with respect to the rotor plane, m/sec
V = rotor forward speed, m/sec
v = induced velocity, m/sec
$\bar{v}$ = mean induced velocity, m/sec
$\bar{x}$ = nondimensional radial position of the blade center of gravity = $\int r dm/mR$
x_β = nondimensional flapping-hinge-offset = r_β/R
β, β_0, β_{1c}, β_{1s} = flapping angles, $\beta = \beta_0 + \beta_{1c}\cos\psi + \beta_{1s}\sin\psi$
$\bar{\beta}_0$ = preconing angle
β = complex flapping angle, $= -\beta_{1s} + j\beta_{1c}$
β_ϵ = steady flapping derivative with respect to angular velocity given by Eq. (14), sec
γ = Lock number = $\rho a c R^4/I$
ϵ = complex angular velocity of the rotor = $-p + jq$, which is normal to the rotor shaft, rad/sec
η_a = nonuniformity parameter given by Eq. (3)
$\eta_{\beta,\theta}$, $\eta_{\beta,\epsilon}$ = complex attenuation factor given by Eq. (7)
θ = pitch angle of the helicopter
θ, θ_0, θ_{1c}, θ_{1s} = blade pitch angles, $\theta = \theta_0 + \theta_{1c}\cos\psi + \theta_{1s}\sin\psi$
Θ = complex pitch angle = $-\theta_{1s} + j\theta_{1c}$
λ = inflow ratio = $(V\sin i + v)/R\Omega$
μ = advance ratio = $V\cos i/R\Omega$
ρ = airdensity, kg sec^2/m^4
σ = solidity = $bc/\pi R$
ϕ = inflow angle = $\tan^{-1}(-U_P/U_T)$
ψ = blade azimuth angle
Ω = rotor rotational speed, rad/sec
ω = swing angular velocity of the rotor, rad/sec

Superscripts

$(^-)$ = conjugate complex quanty of ( )
$(\cdot)$ = time derivative

Subscripts

$(\,)_0$ = steady-state value of ( )
$(\,)_1$ = quantity obtained in the uniform induced flow distribution

Introduction

THE most simple expressions of the rotor damping derivatives for pitch or roll motion in hovering flight were given by Gessow[1] and Amer[2] as $dC_M/d(q/\Omega) = (\partial C_M/\partial\beta_{1c})\, d\beta_{1c}/d(q/\Omega) = (16/\gamma)\partial C_M/\partial\beta_{1c}$ for see-saw rotor system and by Townsent[3] as $dC_M/d(q/\Omega) = -a\sigma/16$ for completely rigid rotor system.‡ The above derivatives sometimes gave overestimated values for the actual rotor system, specifically for hingeless rotor systems in hovering or low μ and low C_T flight.

The theoretical inaccuracies must arise from inadequate assumptions of the induced flow distribution and the treatment of pertinent flapwise motion of the blade. Improvements in the theoretical analyses are surely achievable by introducing the precise induced flow distribution calculated by the Biot-Savart law for the wake vortex system[4] and/or by considering the elastically deformable blade having the flapwise degree of freedom in the extent of higher order modes.[5] This, however, requires more computing time as well as a laborious programing process.

Meanwhile, in the calculation of the nonuniform induced velocity, the momentum theory must be still effective when considering the fact that by applying the momentum theory to each of local pie shaped area on the rotor disk Shupe[5] has obtained a reduction of the lift curve slope similar to Miller's result[6] based on the vortex theory.

For blade flapping motion in hingeless or rigid rotor system, Young[7] has proposed to replace the cantilevered blade with an equivalent offset-hinged blade, which is a rigid

Received November 26, 1973; revision received April 22, 1974.
Index categories: Rotary Wing Aerodynamics; VTOL Handling, Stability, and Control.

*Professor, Institute of Space and Aeronautical Science. Member AIAA.

†Graduate Student.

‡In rigid rotor system the moment is limited to the direct hub moment so that the indirect moment such as the moment derived from the thrust vector times its position vector from the c.g. of the helicopter is excluded here.

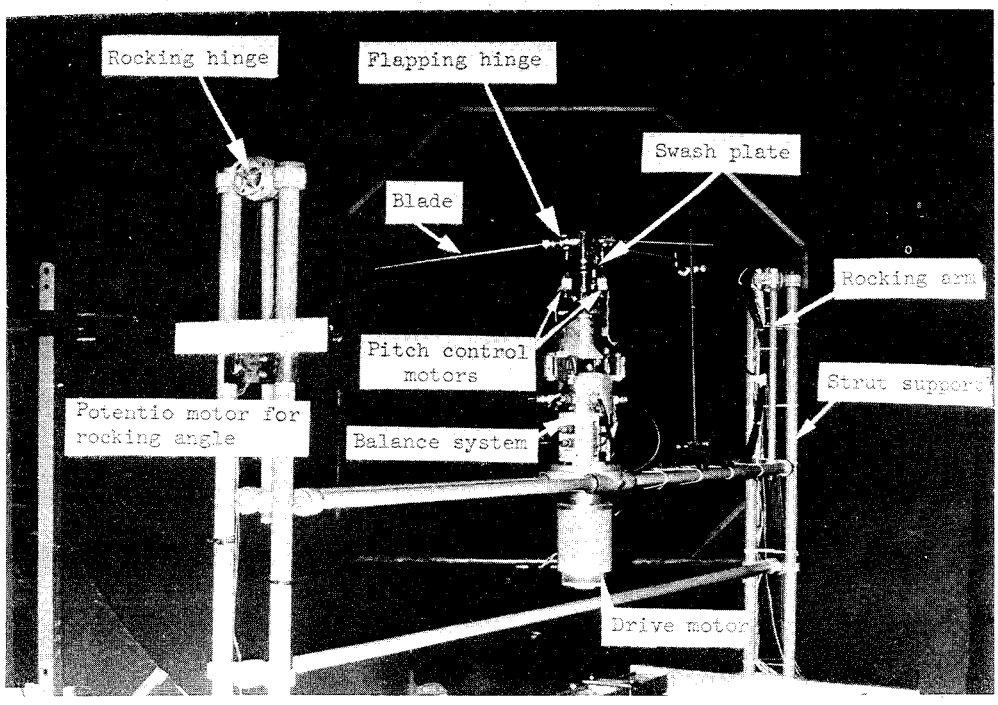

Fig. 1 Test arrangement.

blade with spring restraint at the flapping hinge. As far as the blade motion is concerned, this replacement may be equivalent to including the first mode of the elastic deformation of the hingeless blade. Thus the dynamic response of the system can be treated in a relatively simplified manner and the result is still effective for estimating the hub moments and the related derivatives specifically for a blade having a soft flexible part near the blade root.

Here, all blades used in the present tests were such offset hinged blades, the stiffness of which were so high that the flapwise deflection of the blade resulted only from bending at the hinge restrained by a mechanical spring at the hinge. Then, our attention can be concentrated on the aerodynamic problems of rotor blade without regard to the elastic behavior of the blade. The theoretical calculations based on the simple momentum and blade element theory can then easily be compared with the experimental results.

Experimental Apparatus

Most tests were performed in hovering flight condition. The tests simulating the forward-flight condition were conducted in the open-jet-wind tunnel (3-m-diam) at the Institute of Space and Aeronautical Science, Univ. of Tokyo. The test arrangement is shown in Fig. 1. The model rotor was supported by a frame which allows the free rocking oscillation only in one degree of freedom about the hub without introducing any transversal motion to the hub. The dimensions of the rotors and the operational rotor rpm are listed in Table 1. The test Reynold's number was about 1×10^5 for all blades at blade tip.

The mechanical spring stiffness could be altered by replacing the spring at the flapping hinge with different one. Three different kinds of springs were examined for the present test.

The damping of the rocking motion, which resulted mostly from the rotor aerodynamic damping (with a very small contribution from the mechanical friction of the system) was obtained by sensing the amplitude and the frequency of the oscillation with a photo-electric system.

The hub forces and moments acting on the rotor also were measured by using a balance system installed under the hub which also could swing with the hub and drive motor.

The flapping motion of the blade was sensed by strain gages applied on a leaf spring provided at the flapping hinge, the stiffness of which was negligibly small.

The collective and cyclic pitches were sensed by potentiometers installed on the swash plate together with servomotors which can remotely provide a specified pitch angle of the blade.

Table 1 Model geometry

Items	Model rotors A	B	C
Section	NACA 0012	Clark Y $t/c = 0.14$	Clark Y $t/c = 0.14$
Twist	0	0	0
Materials	Aluminum 52S	Wood	Wood
Radius, m	0.55	0.90	0.75
Chord, m	0.033	0.055	0.050
Solidity, σ	0.0573	0.0584	0.0636
Flapping hinge offset, x_β	0.0818	0.050	0.060
c.g. of the blade, $\bar{x}$	0.241	0.156	0.144
Moment of inertia of the blade, I(kgm sec^2)	0.00118	0.00363	0.00203
Lock number, γ	1.84	7.10	5.62
Rotor dynamic K_1	0.181	0.731	0.571
K_2	0.245	0.996	0.775
parameters, K_3	0.361	1.500	1.16
Spring stiffness, k_β(kg/rad)	0~7.0	0~7.0	0~7.0
Equivalent hinge stiffness, K_β	0.17~2.53	0.0534~6.25	0.0711~7.95
Rotor, rpm	480~600	200~600	200~600

Blade Flapping in Nonuniform Induced Flow Distribution

It is assumed here that the induced velocity has the following inclined funnel-shape distribution:

$$v(x,\psi) = \bar{v}\{1 - (2/3)K_0 + x(K_0 + K_{1c}\cos\psi + K_{1s}\sin\psi)\} \tag{1}$$

where $\bar{v}$ is a mean uniform induced velocity given by $\bar{v} = R\Omega C_T/2(\mu^2 + \lambda^2)^{1/2}$, and K_0, K_{1c}, and K_{1s} are nonuniformity correction factors.[§] The factors can be determined by considering the harmonic balance of the thrust of momentum theory with that of blade element theory.[5,8,9] The result can be given from Appendix A as follows:

$$(\bar{v}/R\Omega)K_{1c} = \eta_a[\theta_{1c}\{1 + (1/4)\mu^2(K_3/K_1)\} - \mu\beta_0(K_2/K_1) - \beta_{1s}\{1 + (1/4)\mu^2(K_3/K_1)\} + (q/\Omega)] \tag{2}$$

$$(\bar{v}/R\Omega)K_{1s} = \eta_a[\theta_{1s}\{1 + (3/4)\mu^2(K_3/K_1)\} + 2\mu\theta_0(K_2/K_1) + \beta_{1c}\{1 - (1/4)\mu^2(K_3/K_1)\} + (p/\Omega) - \mu\lambda(K_3/K_1)]$$

where η_a is a "nonuniformity parameter" given by

$$\eta_a = 1/\{1 + (8/a\sigma)(V/R\Omega) + (16/a\sigma)(\bar{v}/R\Omega)\} \quad \text{for hovering and vertical flight} \tag{3}$$

$$= 1/\{1 + (8/a\sigma)(V/R\Omega) + (16/a\sigma)(\bar{v}/R\Omega)\sin i\} \quad \text{for forward flight}$$

The parameter η_a is strongly affected by the thrust coefficient in hovering and vertical flights but little in forward flight for small i, while for large i the η_a decreases very rapidly as the forward speed increases.

The blade flapping equation of motion can be obtained from the moment balance about the flapping hinge provided with a linear mechanical constraint as follows[10]:

$$k_\beta(\beta - \bar{\beta}_0) = \int dm[\{r_\beta + (r - r_\beta)\cos\beta\}\Omega^2\sin\beta + g\cdot\cos\beta + (r - r_\beta)\{\ddot{\beta} - (\dot{q} + 2p\Omega)\cos\psi - (\dot{p} - 2q\Omega)\sin\psi\}] + \int(1/2)\rho c U^2(c_l\cos\phi - c_d\sin\phi)dr \tag{4}$$

where the left-hand side of the above equation results from the spring constraint and where the first, second, third, and fourth terms in the right-hand side are, respectively, derived from the centrifugal, gravitational, inertia, and aerodynamic forces. Assuming β and $x_\beta = r_\beta/R$ to be small substitute Eqs. (A3) and (A4) into Eq. (4). Then three coupled second-order equations of motion for β_0, β_{1c} and β_{1s} will be obtained from the coefficients of the first three terms in Fourier series of azimuthal angle ψ, i.e., the coefficients of zero, first cosine, and sine components, respectively.

When the induced velocity is constant and uniform, a given "complex cyclic-pitch-input," $\theta = -\theta_{1s} + j\theta_{1c}$, and a specified "complex body-angular-velocity," $\dot{\epsilon} = -p + jq$, yield a complex flapping angle or complex tilt angle of the rotor-tip-path plane, $\beta = -\beta_{1s} + j\beta_{1c}$, of which transfer function is given as follows[10]:

$$\beta_1(s) = [(K_1 + (1/4)K_3\mu^2)\theta(s) - K_2\mu\{2\theta_0 + j\beta_0 + (K_3/K_2)\lambda\}/(s/\Omega) + j(1/4)K_3\mu^2\bar{\beta}_1(s) + (1/4)K_3\mu^2\{\theta(s) + \bar{\theta}(s)\} + \{(s/\Omega) + (K_1 - 2j)\}(\dot{\epsilon}/\Omega)]/\{(s/\Omega)^2 + (K_1 - 2j)(s/\Omega) + (K_\beta - jK_1)\} \tag{5}$$

where subscript 1 for β has been supplemented to show that the result was obtained in the assumption of uniform induced flow distribution, and where $\bar{\beta}$ and $\bar{\theta}$ are complex conjugate quantities of β and θ, respectively.

[§]The term of $-(2/3)K_0$ is derived by taking the $\bar{v}$ equal to the mean velocity over the rotor disk so that a little change in thrust is eventually resulted.

The transient flapping motion is, in general, damped out so rapidly within a few blade rotations that only the steady terminal state of the flapping angle is of our interest in the study of the stability and control characteristics.

When the induced velocity is not uniform, the steady terminal flapping angles for step inputs of the cyclic pitch θ and of the angular velocity, $\dot{\epsilon}/\Omega$, can be given by

$$\beta(\theta) = \eta_{\beta,\theta}\beta_1(\theta) + \eta_{\beta,\dot{\epsilon}}\beta_1(\dot{\epsilon}/\Omega) \tag{6}$$

where $\eta_{\beta,\theta}$ is a "complex attenuation factor" of the flapping angle resulted from the nonuniformity of the induced flow due to the cyclic pitch change, and $\eta_{\beta,\dot{\epsilon}}$ is that due to the body motion; $\beta_1(\theta)$ and $\beta_1(\dot{\epsilon}/\Omega)$ are the steady terminal states of the complex flapping angle in uniformly distributed induced flow.[‡] They are, from Appendix B, respectively, given by

$$\eta_{\beta,\theta} = (1 - \eta_a)/[1 + j\eta_a\{K_1/(K_\beta^2 + K_1^2)^{1/2}\}\exp\{-j\tan^{-1}(-K_1/K_\beta)\}] \tag{7a}$$

$$\eta_{\beta,\dot{\epsilon}} = [1 - \eta_a\{K_1/(K_1^2 + 4)^{1/2}\}\exp\{-j\tan^{-1}(-2/K_1)\}]/[1 + j\eta_a\{K_1/(K_\beta^2 + K_1^2)^{1/2}\}\exp\{-j\tan^{-1}(-K_1/K_\beta)\}] \tag{7b}$$

$$\beta_1(\theta) = \{K_1/(K_1^2 + K_\beta^2)^{1/2}\}\exp\{-j\tan^{-1}(-K_1/K_\beta)\}[\{1 + (1/4)(K_3/K_1)\mu^2\}\theta + (1/4)(K_3/K_1)\mu^2(\bar{\theta} + \bar{\theta} + j\beta_1) - (K_2/K_1)\mu\{2\theta_0 + j\beta_0 + (K_3/K_2)\lambda\}] \tag{8a}$$

$$\beta_1(\dot{\epsilon}/\Omega) = [(K_1^2 + 4)/(K_\beta^2 + K_1^2)]^{1/2}\exp\{j\tan^{-1}(-2/K_1) - j\tan^{-1}(-K_1/K_\beta)\}(\dot{\epsilon}/\Omega) \tag{8b}$$

For fully articulated rotors without offset flapping hinges ($K_\beta = 0$), the attenuation factors become

$$\eta_{\beta,\theta} = 1.0$$
$$\eta_{\beta,\dot{\epsilon}} = [1 - \eta_a[K_1/(K_1^2 + 4)^{1/2}]\exp\{-j\tan^{-1}(-2/K_1)\}]/(1 - \eta_a) \tag{9}$$

for any flight condition. For perfectly rigid rotors ($K_\beta = \infty$), on the other hand, the attenuation factors take the following forms

$$\eta_{\beta,\theta} = 1 - \eta_a$$
$$\eta_{\beta,\dot{\epsilon}} = 1 - \eta_a[K_1/(K_1^2 + 4)^{1/2}]\exp\{-j\tan^{-1}(-2/K_1)\} \tag{10}$$

The above reduction due to the cyclic pitch change was first proposed by Sissing[11] and then extended by Shupe[5] to a simplified correction for the Lock number as follows:

$$\gamma^* = (1 - \eta_a)\gamma$$

Figure 2 shows some examples of $\eta_{\beta,\theta}$ and $\eta_{\beta,\dot{\epsilon}}$ with change of K_β for various C_T or θ_0 in hovering flight and for $V/R\Omega$ in forward flight in which they are almost independent with C_T. As the rigidity or K_β increases from zero to infinity, their absolute values $|\eta_{\beta,\theta}|$ and $|\eta_{\beta,\dot{\epsilon}}|$ decrease monotonically and their phases $\angle\eta_{\beta,\theta}$ and $\angle\eta_{\beta,\dot{\epsilon}}$ decrease once but return to zero after passing a maximum value determined by a proper combination of K_1 and K_β. It can be seen that the reduction of absolute values and phases are predominant for low C_T in hovering flight or low $V/R\Omega$ in forward flight.

[‡]After the present paper had been presented, a referee advised the authors that D. A. Peters published a paper titled "Hingeless Rotor Frequency Response With Unsteady Inflow; Proceedings of the American Helicopter Society and NASA/AMES Research Center Specialists Meeting on Rotorcraft Dynamics, Moffet Field, Calif., Feb. 13-15, 1974, in which Peters discussed the nonuniform, unsteady induced flow effects on the hingeless rotor frequency response. However, he laid stress on the unsteadiness of the inflow perturbation rather than the nonuniformity. In the present paper the unsteady term in momentum contribution on the lift had been neglected because, unlike the blade flutter, the frequency of actual rotor shaft motion or helicopter body motion was considered to be sufficiently small.

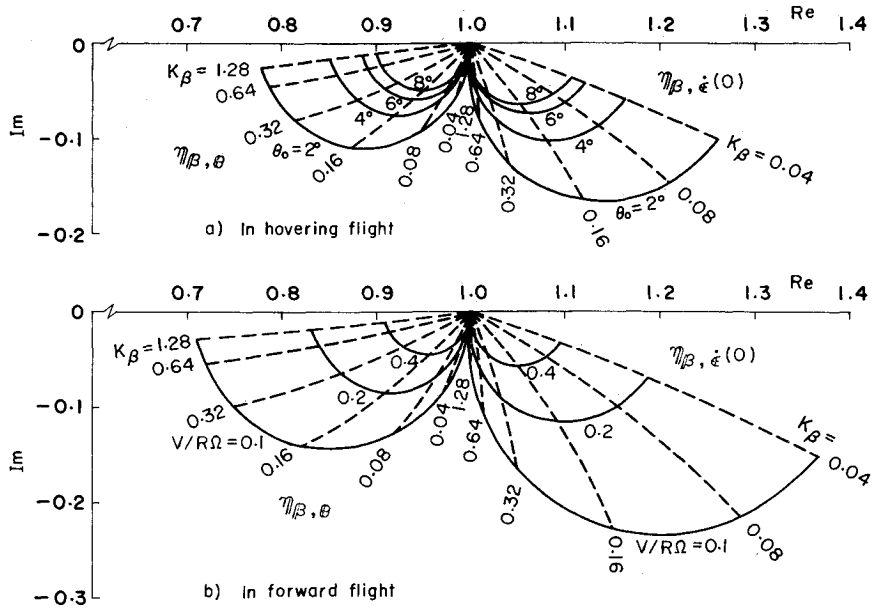

Fig. 2 Examples of attenuation factors for blade flapping ($K = 0.18$).

Figure 3 shows experimental verification on the effect of K_β in the flapping response due to the cyclic pitch input in hovering flight. The test has been conducted for various K_β depending on different combinations of Lock number and the stiffness of spring provided at the flapping hinge. It will be observed that the above described simple theory based on the nonuniform induced flow shows good coincidence with the experimental results except for the phase at low K_β. The phase discrepancies in low K_β must be caused from not only by the imperfection of the preceding simple theory but also from a poor estimation of K_β due to inadequate arrangement of the mechanical spring in the model rotor.

Rotor Response for Sinusoidal Rocking Motion

Suppose that the body angular velocity $\dot{\epsilon}$ is given by a forced sinusoidal motion such as

$$\dot{\epsilon}/\Omega = (\dot{\epsilon}_0/\Omega)\exp(j\omega t) \tag{11}$$

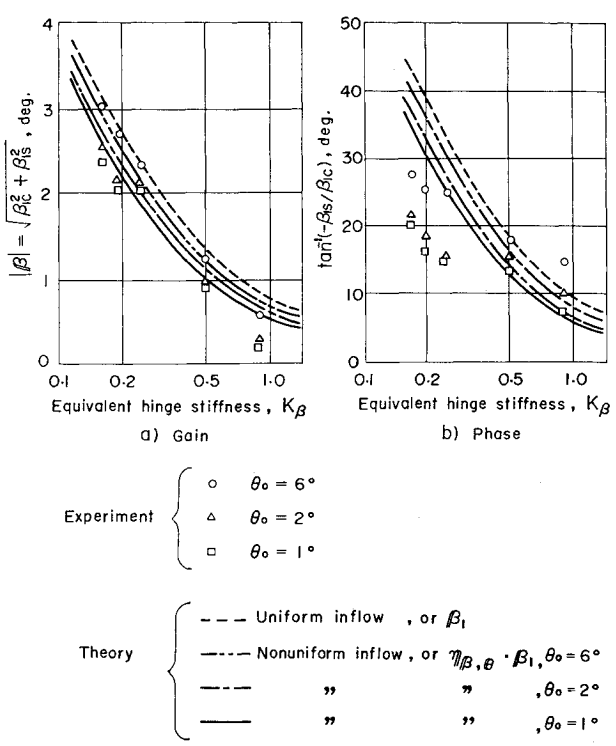

Fig. 3 Flapping response by pitch input in hovering flight ($\theta_{1s} = -4°, \gamma = 1.84$.

The frequency of the motion may be considered so small that the unsteady aerodynamic effects can be neglected. Hence the response of the tip path place can, from Appendix B, be given by

$$\beta(\dot{\epsilon}) = \eta_{\beta,\dot{\epsilon}}(\omega)\cdot\beta_{\dot{\epsilon}}(\omega)\cdot\dot{\epsilon}/\Omega \tag{12}$$

where

$$\eta_{\beta,\dot{\epsilon}}(\omega) = \{1 - [\eta_a/(1 + \{(\omega/\Omega) - 2\}^2/K_1^2)^{1/2}] \exp[-j\tan^{-1}\{((\omega/\Omega) - 2)/K_1\}]\}/\{1 + j\eta_a[(K_1/(\{K_\beta + 2(\omega/\Omega) - (\omega/\Omega)^2\}^2 + K_1^2\{1 - (\omega/\Omega)\}^2)^{1/2}] \exp[-j\tan^{-1}\{-K_1(1 - (\omega/\Omega))/(K_\beta + 2(\omega/\Omega) - (\omega/\Omega)^2)\}]\} \tag{13}$$

$$\beta_{\dot{\epsilon}}(\omega) = \{[K_1^2 + (\omega/\Omega - 2)^2]^{1/2}/[\{K_\beta + 2(\omega/\Omega) - (\omega/\Omega)^2\}^2 + K_1^2\{1 - (\omega/\Omega)\}^2]^{1/2}\} \exp[j\tan^{-1}\{(\omega/\Omega - 2)/K_1\} - j\tan^{-1}\{-K_1(1 - \omega/\Omega)/(K_\beta + 2\omega/\Omega - (\omega/\Omega)^2)\}] \tag{14}$$

Figure 4 shows the preceding attenuation factor for various ω and θ_0. It is interesting to find that the factor changes with ω/Ω and the rate of change is more predominant for lower θ_0 as well as lower stiffness of the rotor blade. For slow body motion or $\omega/\Omega \ll 1$ and usual operational range of C_T or $\eta_a \ll 1$, the absolute value of $\eta_{\beta,\dot{\epsilon}}(\omega)$ may not be approximated by that of $\eta_{\beta,\theta}$ but the phase of $\eta_{\beta,\dot{\epsilon}}(\omega)$ is nearly equal to that of $\eta_{\beta,\theta}$ in low ω.

When only the forced sinusoidal pitching oscillation is under consideration

$$\dot{\Theta}/\Omega = \Theta_0(\omega/\Omega)\sin(\omega t)$$

$$\text{or} \quad \dot{\epsilon}/\Omega = (1/2)\Theta_0(\omega/\Omega)\{\exp(j\omega t) - \exp(-j\omega t)\} \tag{15}$$

the sinusoidal flapping motion becomes

$$\beta(\dot{\epsilon}/\Omega) = (1/2)\Theta_0(\omega/\Omega)\{\eta_{\beta,\dot{\epsilon}}(\omega)\beta_{\dot{\epsilon}}(\omega)e^{j\omega t} - \eta_{\beta,\dot{\epsilon}}(-\omega)\beta_{\dot{\epsilon}}(-\omega)e^{-j\omega t}\} \tag{16}$$

Equation (16) gives an elliptic motion in the β plane, that is to say, the vector β in the complex plane, which is the projection of a normal vector of the rotor tip path plane, moves along the elliptic orbit in the same period as that of rocking motion, as shown in Fig. 5.** If the absolute value of either one of vector $\beta_{\dot{\epsilon}}(\omega)$ or $\beta_{\dot{\epsilon}}(-\omega)$ in Eq. (16) is

**Recently, very similar diagram of β was obtained for the sinusoidal cyclic pitch input in Ref. 12.

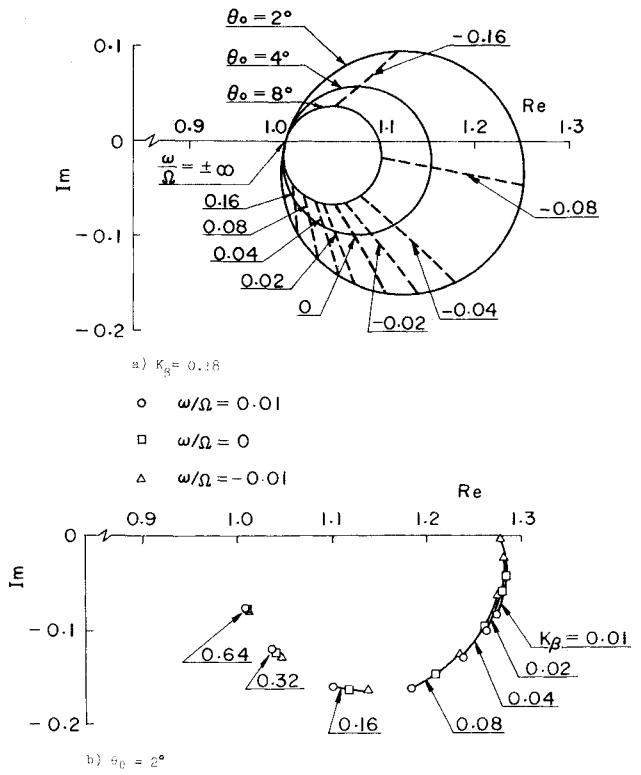

Fig. 4 Attenuation factor $\eta_{\beta,\dot{\epsilon}}(\omega)$ for sinusoidal rocking motion in hovering flight ($K_\beta = K_1 = 0.18$).

very small the orbit will be nearly circle, whereas if its ratio, $|\beta_{\dot{\epsilon}}(\omega)|/|\beta_{\dot{\epsilon}}(-\omega)|$, approaches to one the eccentricity of the ellipse becomes large. The above ratio depends on the combination of the K_1 and K_β.

The rotation of the vector $b(\dot{\epsilon}/\Omega)$ is thus governed by the larger one of either $\beta(\omega)$ or $\beta(-\omega)$. It will be observed from Fig. 5 that as the K_β increases the major axis of the ellipse tends to tilt from the imaginary axis to the real axis of the complex β-plane and simultaneously to shrink to zero.

In Fig. 5 the theoretically obtained vectors β due to pitching oscillation are plotted for the cases of uniform inflow distribution and nonuniform inflow distribution corrected by the attenuation factors $\eta_{\beta,\theta}$, $\eta_{\beta,\dot{\epsilon}}(0)$ and $\eta_{\beta,\dot{\epsilon}}(\omega)$ though there is no any positive propriety to adopt $\eta_{\beta,\theta}$ for the nonuniform correction. The sizes of the ellipse are different for respective factor but the phase are almost unchanged in the usual operational range of the rotor. Experimental results are also shown in Fig. 5 in normalized form based on the amplitude of the rocking motion in each cycle. They are very close to the ellipse corrected for nonuniform induced flow distribution by $\eta_{\beta,\theta}$ rather than $\eta_{\beta,\dot{\epsilon}}(\omega)$ or $\eta_{\beta,\dot{\epsilon}}(0)$. The most important difference among these factors is that the absolute value of $\eta_{\beta,\theta}$ is less than 1 while those of remainings are larger than 1 in usual operational range of ω/Ω. The experimental test shows that the damping is still overestimated by the present simple theory though the three-dimensional effect is counted by taking $B = 0.97$. Takazawa has shown that the variation of relative positions between the rotor blades and their shed vortices in the wake due to the rotor motion must be taken into acount for the estimation of the damping.[4] If we wish to use the present simple momentum theory rather than the more complex vortex theory, it may be said that the pitch damping should be corrected by the factor $\eta_{\beta,\theta}$ rather than $\eta_{\beta,\dot{\epsilon}}(\omega)$.

Radial vectors in each ellipse designated by $\beta_{\max|\dot{\epsilon}|}$ in Fig. 5 show azimuthal position of β at which the rocking velocity is maximum. The meaning of these radial vectors on the damping in rocking motion will be described in later.

Damping Moment Derivative

The pitch damping derivative of the hub moment will be given by

$$dC_{M_Y}/d(q/\Omega) = \partial C_{M_Y}/\partial(q/\Omega) + (\partial C_{M_Y}/\partial\beta_{1c})d\beta_{1c}/d(q/\Omega) + (\partial C_{M_Y}/\partial\beta_{1s})d\beta_{1s}/d(q/\Omega) \quad (17)$$

in which the first term results from the direct shear force acting on the flapping hinge and the second and third terms are obtained from the indirect terms due to the blade flapping motion following the body motion.†† The blade element theory provides their expressions as follows:

††Since the rocking motion has been considered sinusoidal here, any damping which might be created from the driving motor through the resistive work opposing to the Coriolis force can be neglected as small quantities.

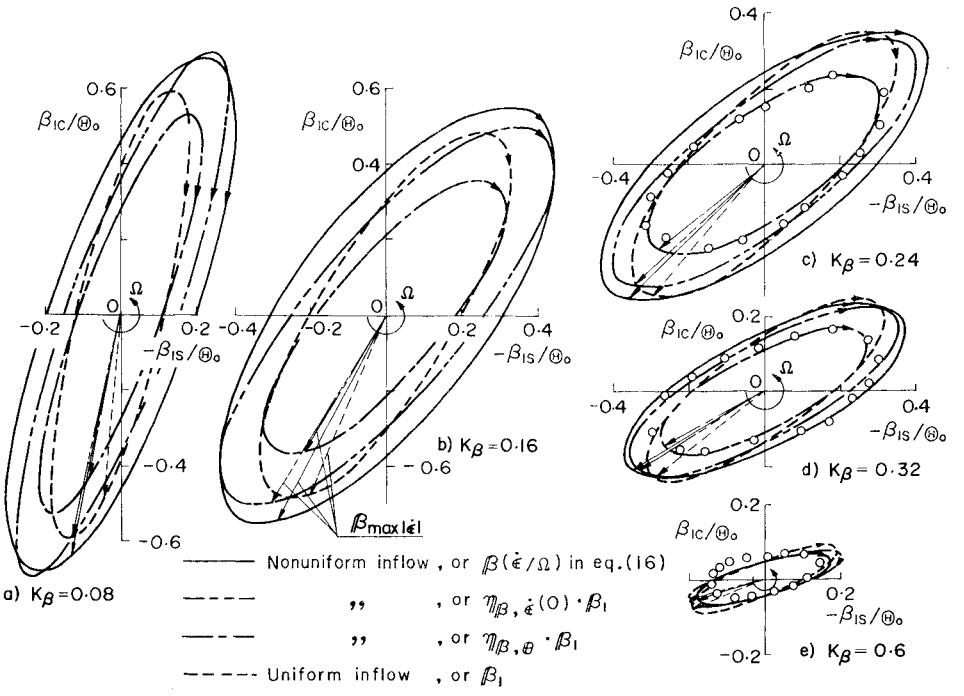

Fig. 5 Flapping for sinusoidal hub motion in hovering flight ($K_1 = 0.16, \theta_0 = 2°, \gamma = 1.84$).

$$\partial C_{M_Y}/\partial(q/\Omega) = -x_\beta(1/2)a\sigma\{(1-\eta_a)(1/6)B^3\}$$

$$\partial C_{M_Y}/\partial\beta_{1c} = -(1/2)(bm/\rho SR)\{x_\beta\bar{x} + k_\beta/m(R\Omega)^2\} \quad (18)$$

$$\partial C_{M_Y}/\partial\beta_{1s} = x_\beta(1/2)a\sigma[(1/6)B^3 + (1/8)B\mu^2 - \eta_a\{(1/6)B^3 + (1/24)B^3\mu^2(K_3/K_1)\}]$$

$$d\beta_{1c}/d(q/\Omega) = -\eta_{\beta s}K_1(2+K_\beta)/(K_1^2 + K_\beta^2 - (1/4)K_1K_3\mu^2) - \eta_{\beta c}(K_1^2 - 2K_\beta)/(K_1^2 + K_\beta^2 + (1/4)K_1K_3\mu^2) \quad (19)$$

$$d\beta_{1s}/d(q/\Omega) = \eta_{\beta c}K_1(2+K_\beta)/(K_1^2 + K_\beta^2 - (1/4)K_1K_3\mu^2) - \eta_{\beta s}(K_1^2 - 2K_\beta)/(K_1^2 + K_\beta^2 + (1/4)K_1K_3\mu^2)$$

where $\eta_{\beta c}$ and $\eta_{\beta s}$ are, respectively, the imaginary and negative real parts of $\eta_{\beta,\dot{\epsilon}}$ such as $\eta_{\beta,\dot{\epsilon}}(\omega) = -\eta_{\beta s} + j\eta_{\beta c}$.

The first term in Eq. (17) is directly proportional to hinge offset, x_β, and the solidity σ. The second term has a peak at some K_β. The third term is a crossed term and is generally small. Figure 6a shows examples of the pitch damping derivative calculated for various x_β and K_β combinations. Figure 6b shows experimental results obtained from the rocking motion of the rotor for various K_β. The pitch damping derivatives in the sinusoidal rocking motion have been obtained from $dC_M/d(q/\Omega) = \ln|H(t_2)/\theta(t_1)|I_s\omega/\pi\rho SR^3\Omega$, where t_2 and t_1 are time spanned one cycle and I_s is the moment of inertia of the system. In the present rotor system this derivative is, from the blade element theory, approximated by

$$dC_{M_Y}/d(q/\Omega) \doteqdot \partial C_{M_Y}/\partial(q/\Omega) + (\partial C_{M_Y}/\partial\beta_{1c})\beta_{1c,\max q} + (\partial C_{M_Y}/\partial\beta_{1s})\beta_{1s,\max q} \quad (20)$$

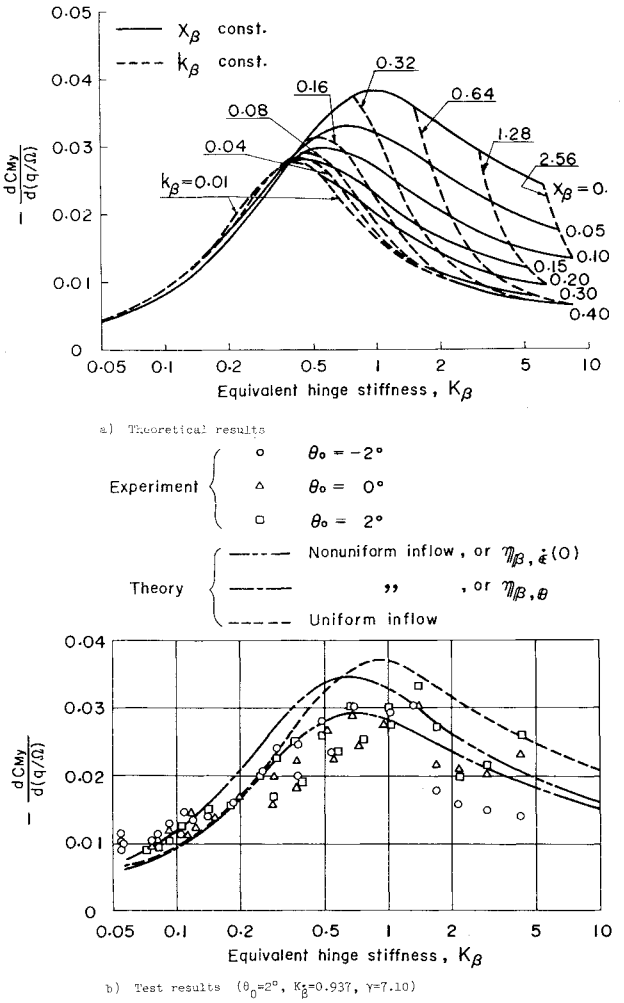

Fig. 6 Examples of pitch damping derivative in hovering flight a) theoretical results, b) test results ($\theta_0 = 2°$, $K_\beta = 0.937$, $\gamma = 7.10$).

where $\beta_{1c,\max q}$ and $\beta_{1s,\max q}$ are β_{1c} and β_{1s} at the maximum pitching velocity and are, respectively, given by

$$\beta_{1c,\max q} = [\{\eta_{\beta,\dot{\epsilon}}(\omega)\cdot\beta_{\dot{\epsilon}}(\omega) - \overline{\eta_{\beta,\dot{\epsilon}}(\omega)}\,\overline{\beta_{\dot{\epsilon}}(\omega)}\} - \{\eta_{\beta,\dot{\epsilon}}(-\omega)\beta_{\dot{\epsilon}}(-\omega) - \eta_{\beta\dot{\epsilon}}(-\omega)\beta_{\dot{\epsilon}}(-\omega)\}]/4j \quad (21)$$

$$\beta_{1s,\max q} = [\{\eta_{\beta,\dot{\epsilon}}(\omega)\beta_{\dot{\epsilon}}(\omega) + \overline{\eta_{\beta,\dot{\epsilon}}(\omega)}\cdot\overline{\beta_{\dot{\epsilon}}(\omega)}\} - \{\eta_{\beta\dot{\epsilon}}(-\omega)\beta_{\dot{\epsilon}}(-\omega) - \eta_{\beta,\dot{\epsilon}}(-\omega)\beta_{\dot{\epsilon}}(-\omega)\}]/4$$

It will be observed that for small K_β the test results are concentrated near the theoretical value corrected by $\eta_{\beta,\dot{\epsilon}}(0)$, while for large K_β near the peak value of the damping they are rather distributed around the value corrected by $\eta_{\beta,\theta}$.

It will be appreciated from Eq. (20) that the maximum damping is affected by a combination of $\beta_{1c,\max q}$ and $\beta_{1s,\max q}$ or the radial vectors, $\beta_{\max\dot{\epsilon}}$, shown in Fig. 5. In usual rotor configuration the second direct term is predominant over other terms so that the larger $\beta_{1c,\max q}$ gives better damping.

In forward flight the μ affects to improve the pitch damping and to reduce the roll damping. This is, as shown in Fig. 7, due to the flapping or tilt response of the rotor tip path plane. Figure 8 shows examples of pitch damping obtained from the wind tunnel tests for A blades in Table 1. It is also noticed there that the tests show good coincidence with the theory based on the nonuniform inflow distribution.

Cross coupling derivatives, $dC_{MY}/d(p/\Omega)$ and $dC_{MX}/d(q/\Omega)$, can be given by similar form as Eq. (17)

$$dC_{M_Y}/d(p/\Omega) = \partial C_{M_Y}/\partial(p/\Omega) + (\partial C_{M_Y}/\partial\beta_{1c})d\beta_{1c}/d(p/\Omega) + (\partial C_{M_Y}/\partial\beta_{1s})d\beta_{1s}/d(p/\Omega) \quad (22)$$

$$dC_{M_X}/d(q/\Omega) = \partial C_{M_X}/\partial(q/\Omega) + (\partial C_{M_X}/\partial\beta_{1c})d\beta_{1c}/d(q/\Omega) + (\partial C_{M_X}/\partial\beta_{1s})d\beta_{1s}/d(q/\Omega)$$

where newly introduced coefficients are given by

$$-\partial C_{M_Y}/\partial(p/\Omega) = \partial C_{M_X}/\partial(q/\Omega) = (bm/\rho SR)x_\beta\bar{x}$$

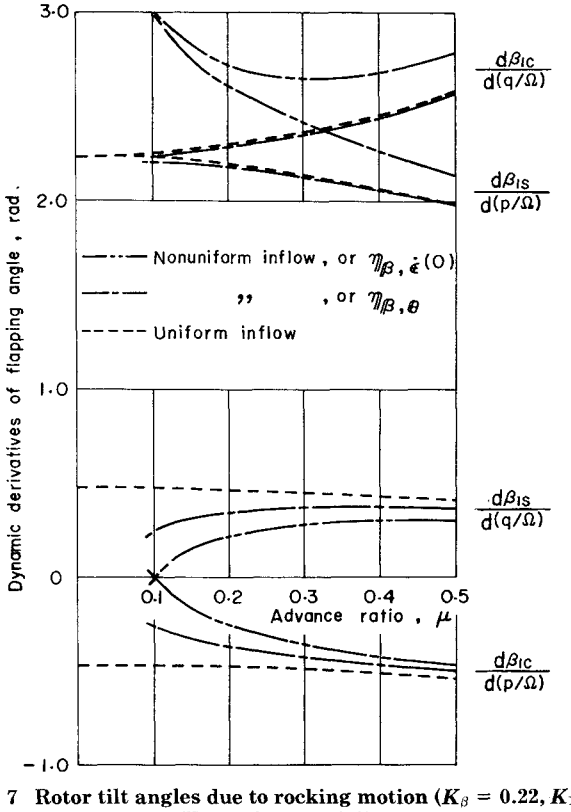

Fig. 7 Rotor tilt angles due to rocking motion ($K_\beta = 0.22$, $K_1 = K_\beta = 0.937$, $\gamma = 9.8$).

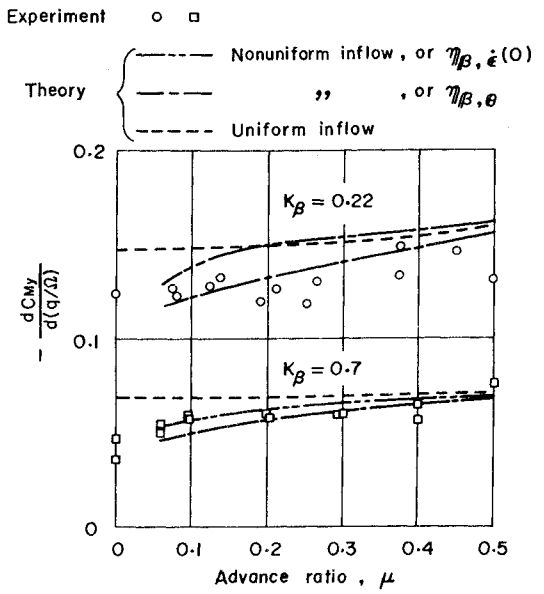

Fig. 8 Pitch damping in forward flight ($\theta_0 = 4°$, $K_\beta = 0.18$, $\gamma = 1.84$).

$$\partial C_{M_X}/\partial\beta_{1c} = -\partial C_{M_Y}/\partial\beta_{1s} \qquad (23)$$
$$\partial C_{M_X}/\partial\beta_{1s} = \partial C_{M_Y}/\partial\beta_{1c}$$

$$d\beta_{1c}/d(p/\Omega) = \eta_{\beta_s}(K_1^2 - 2K_\beta)/(K_1^2 + K_\beta^2 - (1/4)K_1K_3\mu^2) - \eta_{\beta_c}K_1(2 + K_\beta)/(K_1^2 + K_\beta^2 + (1/4)K_1K_3\mu^2) \qquad (24)$$

$$d\beta_{1s}/d(p/\Omega) = -\eta_{\beta_c}(K_1^2 - 2K_\beta)/(K_1^2 + K_\beta^2 - (1/4)K_1K_3\mu^2) - \eta_{\beta_s}K_1(2 + K_\beta)/(K_1^2 + K_\beta^2 + (1/4)K_1K_3\mu^2)$$

Figures 9 and 10 show the above cross coupling derivatives for the rotor in hovering and forward flight, respectively. As the K_β increases, the cross coupling derivatives become appreciable so that the cross coupling moments are induced. As the μ increases, the coupling effects are slightly reduced.

Conclusion

Experimental tests for pitch or roll damping of helicopter rotor have been conducted in wind tunnel by using model rotors with different combination of Lock number, flapping hinge offset, and its hinge constrained stiffness. A theoretical method of estimation based on the simple momentum theory has been developed by taking account of the nonuniformity of the induced flow distribution which is predominant for low C_T and low μ flight in rigid rotor system. Three attenuation factors for the flapping motion

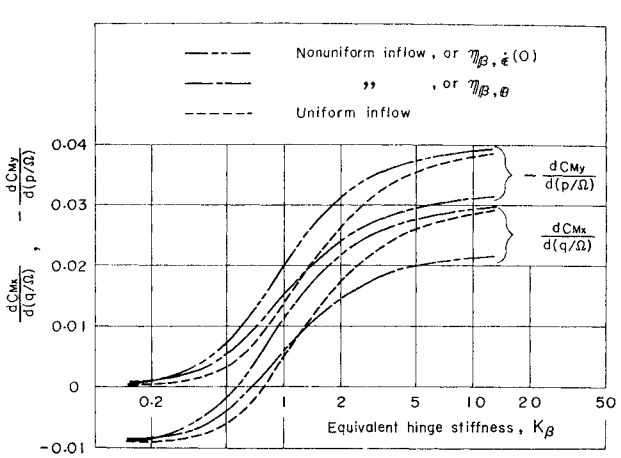

Fig. 10 Cross coupling terms in forward flight, $dC_{My}/d(p/\Omega) \sim \mu K_{\beta=0.22,K1} = K_\beta = 0.937, \gamma = 9.8$).

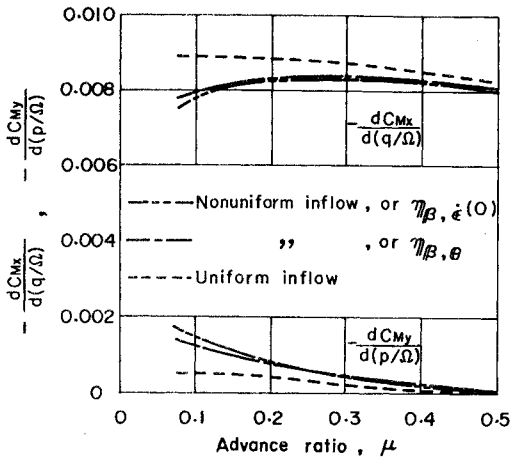

Fig. 9 Cross coupling terms in hovering flight ($\theta_0 = 2°$, $K_1 = K_\beta = 0.937$, $\gamma = 9.8$).

have been derived from the theory. The test result showed good coincidence with these factors in phase but not always so in amplitude. It was found that the attenuation factor for the cyclic pitch response, $\eta_{\beta,\theta}$, gave the best correction over the others for the estimation of the rotor damping.

The blade flapping behavior during rocking motion has been analytically estimated and represented by an elliptic orbit in the β plane. The eccentricity of ellipse, the length of and the tilt angle of the major axis are strongly dependent on the equivalent stiffness of the blade, K_β. The direct damping term and the coupled moment are related to the radial vector at the maximum rocking angular velocity, $\beta_{\max}\dot{\epsilon}$. The experimental test results which have been conducted for a few examples have shown good coincidence with the above simple theory.

Appendix A: Nonuniformity Parameter

Let us consider a reaction force acting on a pie shaped area shown in Fig. 11a, which is generated by a rotor blade

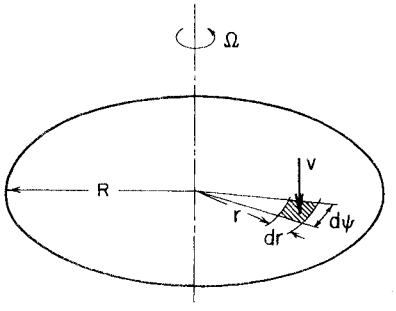

a) Pie shaped area

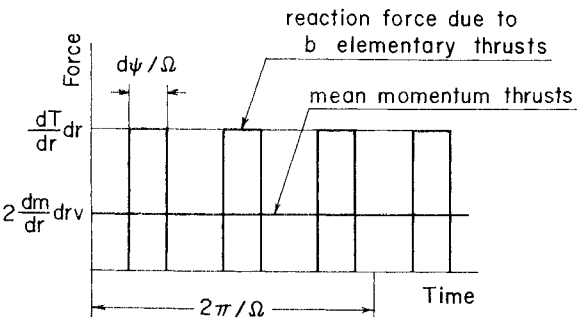

b) Force balance between b elementary thrusts and mean momentum thrust

Fig. 11 Pulsating forces and momentum thrust over pie shaped area.

rotating on the rotor disk. In a very idealized case where the blade remains on the rotor disk, the reaction force is created only when a blade element passes through just on the pie shaped area and the contribution due to the remaining part of the blade can be discarded. Thus, within the time of one revolution of the rotor, $2\pi/\Omega$, the pie shaped area will subject to a series of b pulsating forces each height and width of which are respectively given by an elementary thrust $(dT/dr)dr$ and time $d\psi/\Omega$ as shown in Fig. 11b. It may be considered that these pulsating forces can be balanced by a mean momentum thrust over that area as follows[5,9]:

$$b(dT/dr)dr(d\psi/\Omega) = 2(dm/dr)vdr(2\pi/\Omega)d\psi$$

where $(dm/dr)dr$ is the mass flow through the pie shaped area induced by the reaction forces. Thus the above relation yields

$$(b/2\pi)(dT/dr)drd\psi = 2\rho r(V + v)vdrd\psi \quad \text{for hovering and vertical flights} \tag{A1}$$

$$= 2\rho r[(V\cos i)^2 + (V\sin i + \dot{v})^2]^{1/2}vdrd\psi \quad \text{for forward flight}$$

It has been assumed here that in forward flight the parallel flow on the pie shaped element also participated in the generation of the momentum thrust.

From the blade element theory, the elementary thrust can be given by

$$dT/dr = (1/2)\rho ac(\theta U_T^2 + U_T U_P) \tag{A2}$$

where

$$U_T = R\Omega(x + \mu\sin\psi)$$

$$U_P = -R\Omega[\mu\tan i + (\bar{v}/R\Omega)\{1 - (2/3)K_0 + x(K_0 + K_{1c}\cos\psi + K_{1s}\sin\psi) + \mu(\beta_0 + \beta_{1c}\cos\psi + \beta_{1s}\sin\psi)\cos\psi + x\{-(\beta_{1c} + p/\Omega)\sin\psi + (\beta_{1s} - q/\Omega)\cos\psi\}] \tag{A3}$$

$$\beta = \beta_0 + \beta_{1c}\cos\psi + \beta_{1s}\sin\psi$$
$$\theta = \theta_0 + \theta_{1c}\cos\psi + \theta_{1s}\sin\psi \tag{A4}$$

The blade flapping motion and the rotational or rocking motion of the rotor have been taken into account in the above expressions because they are important factors to decide the nonuniform distribution of the induced velocity. Combining Eqs. (A1–A3) and assuming that the correction factors are represented at $x = 3B/4$, Eqs. (2) and (3) will approximately be derived. The factor K_0 will be left out of consideration in the present analysis.

Appendix B: Attenuation Factor

When the induced velocity is not uniform, the flapping equation of motion (5) can be modified by

$$\beta(s) = [(1 - \eta_a)\{(K_1 + (1/4)K_3\mu^2)\theta(s) - K_2\mu\{2\theta_0 + j\beta_0 + (K_3/K_2)\lambda\}/(s/\Omega) + (1/4)K_3\mu^2(\theta(s) + \bar{\theta}(s) + j\bar{\beta}_1(s)\} + \{(s/\Omega) + (K_1 - 2i - \eta_a K_1)\}\dot{\epsilon}(s)/\Omega]/[(s/\Omega)^2 + (K_1 - 2j)(s/\Omega) + \{K_\beta - (1 - \eta_a)jK_1\}] \tag{B1}$$

Then, step inputs of θ and $\dot{\epsilon}$ result the following steady terminal state:

$$\beta = \lim_{s\to 0} s\beta(s)$$
$$= [(1 - \eta_a)\{(K_1 + (1/4)K_3\mu^2)\theta + (1/4)K_3\mu^2(\theta + \bar{\theta} + j\beta_1) - K_2\mu(2\theta_0 + j\beta_0 + (K_3/K_2)\lambda)\} + (K_1 - 2i - \eta_a K_1)\cdot(\dot{\epsilon}/\Omega)]/\{K_\beta - (1 - \eta_a)jK_1\} \equiv \eta_{\beta,\theta}\beta_1(\theta) + \eta_{\beta,\dot{\epsilon}}\beta_1(\dot{\epsilon}/\Omega) \tag{B2}$$

where $\eta_{\beta,\theta}$, $\eta_{\beta,\dot{\epsilon}}$, $\beta_1(\theta)$ and $\beta_1(\dot{\epsilon}/\Omega)$ are, respectively, given by Eqs. (7a–8b).

For sinusoidal input of body angular motion such as

$$\dot{\epsilon}/\Omega = (\dot{\epsilon}_0/\Omega)\exp(j\omega t) \tag{B3}$$

the terminal flapping motion becomes

$$\beta(\dot{\epsilon}/\Omega) = [\{1 - \eta_a(K_1/(K_1^2 + \{(\omega/\Omega) - 2\}^2)^{1/2}] \times \exp[-j\tan^{-1}\{((\omega/\Omega) - 2)/K_1\}]\}/\{1 + j\eta_a[K_1/(\{K_\beta + 2(\omega/\Omega) - (\omega/\Omega)^2\}^2 + K_1^2\{1 - (\omega/\Omega)\}^2)^{1/2}] \times \exp[-j\tan^{-1}\{-K_1(1 - \omega/\Omega)/(K_\beta + 2(\omega/\Omega) - (\omega/\Omega)^2)\}]\}] \tag{B4}$$
$$\times [(K_1^2 + \{(\omega/\Omega) - 2\}^2)^{1/2}/(\{K_\beta + 2(\omega/\Omega) - (\omega/\Omega)^2\}^2 + K_1^2\{1 - (\omega/\Omega)^2\})^{1/2}] \exp[j\tan^{-1}\{(\omega/\Omega - 2)/K_1\} - j\tan^{-1}\{-K_1(1 - (\omega/\Omega))/(K_\beta + 2(\omega/\Omega) - (\omega/\Omega)^2)\}](\dot{\epsilon}_0/\Omega)\exp(j\omega t) \equiv \eta_{\beta,\dot{\epsilon}}(\omega)\cdot\beta_{\dot{\epsilon}}(\omega)\cdot\dot{\epsilon}/\Omega$$

where $\eta_{\beta,\dot{\epsilon}}(\omega)$ and $\beta_{\dot{\epsilon}}(\omega)$ are given Eqs. (13) and (14), respectively.

References

[1]Gessow, A. and Amer, K. B., "An Introduction to the Physical Aspects of Helicopter Stability," TN 1982, 0000 NACA.

[2]Amer, K. B., "Theory of Helicopter Damping in Pitch or Roll and a Comparison With Flight Measurements," TN 2136, Oct. 1950, NACA.

[3]Townsent, M. W., "Stability and Control of Unducted Stand-On Helicopter Preliminary Theoretical and Flight Test Results," Dept. of Aerospace Engineering, Princeton University, Rept. 404, Nov. 1957, Princeton, N.J.

[4]Takazawa, K., "On the Aerodynamic Damping Moment in Pitch of a Rigid Helicopter Rotor in Hovering. Part II. Analytical Phase," *Transactions of the Japan Society for Aeronautical and Space Sciences*, Vol. 16, No. 32, 1973, pp. 77–101.

[5]Shupe, N. K., "A Study of the Dynamic Motions of Hingeless Rotored Helicopters," Tech. Rept. ECOM-3323, Aug. 1970, AD 713402,

[6]Miller, R. H., "Rotor Blade Harmonic Air Loading," *AIAA Journal*, Vol. 2, No. 7, July 1964, pp. 1254–1269.

[7]Young, M. I., "A Simplified Theory of Hingeless Rotors With Application to Tandem Helicopters," *Proceedings of the Eighteenth Annual National Forum of the American Helicopter Society*, May 1952 pp. 38–45.

[8]Stewart, W. and Sissingh, G. J., "Dynamic Longitudinal Stability Measurements on A Single-Rotor Helicopter (Hoverfly MK.I)," R & M 2505, Feb. 1948, Aeronautical Research Council, London, England.

[9]Curtiss, H. C. and Shupe, N. K., "A Stability and Control Theory for Hingeless Rotors," presented at the 29th Annual National V/STOL Forum of the American Helicopter Society, May 1971.

[10]Azuma, A., "Dynamic Analysis of the Rigid Rotor System," *Journal of Aircraft*, Vol. 4, No. 3, May–June 1967, pp. 203–209.

[11]Sissingh, G. J., "The Effect of Induced Velocity Variation on Helicopter Rotor Damping in Pitch or Roll," Tech. Paper, C.P. 101, 1952, Aeronautical Research Council, London, England.

[12]Curtiss, H. C., Jr., "Complex Coordinates in Near Hovering Rotor Dynamics," *Journal of Aircraft*, Vol. 10, No. 5, May 193, pp. 289–296.